Biomaterials 31 (2010) 7070–7077

Contents lists available at ScienceDirect

Biomaterials

journal homepage: www.elsevier.com/locate/biomaterials

Customizable, multi-functional fluorocarbon nanoparticles for quantitative *in vivo* imaging using ^{19}F MRI and optical imaging

Mangala Srinivas [a], Luis J. Cruz [a], Fernando Bonetto [a], Arend Heerschap [b], Carl G. Figdor [a], I. Jolanda M. de Vries [a,*]

[a] Department of Tumor Immunology, Radboud University Nijmegen Medical Center, Nijmegen, The Netherlands
[b] Department of Radiology, Radboud University Nijmegen Medical Center, Nijmegen, The Netherlands

ARTICLE INFO

Article history:
Received 11 May 2010
Accepted 25 May 2010
Available online 20 June 2010

Keywords:
MRI
19F MRI
Quantitative cell tracking
In vivo fluorescence imaging
Multimodal imaging agents

ABSTRACT

Monitoring cell trafficking *in vivo* noninvasively is critical to improving cellular therapeutics, drug delivery, and understanding disease progression. *In vivo* imaging, of which magnetic resonance imaging (MRI) is a key modality, is commonly used for such monitoring. ^{19}F MRI allows extremely specific detection and quantification of cell numbers directly from *in vivo* image data, longitudinally and without ionizing radiation. We used fluorocarbons previously used in blood substitutes and imaging agents for ultrasound and computed tomography to synthesize monodisperse nanoparticles that are stable at 37 °C and can be frozen for storage. These large ^{19}F labeling compounds are insoluble in aqueous environments and often emulsified, typically forming emulsions unsuitable for long-term storage. Instead, we used a non-toxic polymer already in clinical use, poly(D,L-lactide-co-glycolide), to encapsulate a range of ^{19}F compounds. These nanoparticles can be customized in terms of content (imaging agent, fluorescent dye, drug), size (200–2000 nm), coating (targeting agent, antibody) and surface charge (−40 to 30 mV). We added a fluorescent dye and antibody to demonstrate the versatility of this modular imaging agent. These nanoparticles are adaptable to multimodal imaging, although here we focused on MRI and fluorescence imaging. Here, we imaged primary human dendritic cells, as used in clinical vaccines.

1. Introduction

Cellular therapeutics can be monitored using noninvasive imaging techniques, to optimize the route of delivery, cell treatments, migration, proliferation, localization, dosage and other factors. Magnetic resonance imaging (MRI) is a key imaging modality due to its noninvasive nature, intrinsic anatomic contrast, high resolution and also because it does not use ionizing radiation. Other techniques in use include positron emission tomography (PET), ultrasound and computed tomography (CT). However, all of these imaging modalities have inherent limitations, and thus the use of multimodal imaging with multimodal imaging agents to label cells is gaining ground.

Perfluorocarbons (PFCs) have been in clinical use for a few decades. These compounds were initially developed as commercial blood substitutes, and have since been adapted for CT and ultrasound [1,2]. PFCs have been used for drug delivery [3] and *in vivo* oximetry [reviewed in [4]] especially for tumor hypoxia measurements [5]. More recently, PFCs have been developed for cell tracking and quantification using ^{19}F magnetic resonance imaging (MRI) [6–8]. Such *in vivo* imaging can allow for dynamic monitoring of cellular therapeutics after transfer, enabling the study of localization, quantity and viability. Knowledge of these parameters will help optimize the route of delivery, dosage and other factors. A key limitation in the use of PFCs is their fluorophilicity, which renders them largely insoluble and potentially toxic in aqueous environments. Emulsification with lipid surfactants has typically been the solution [9,10]. However, these emulsions often proved unstable and difficult to use, for example, the FDA-approved blood substitute Fluosol-DA (Green Cross Corp., Osaka, Japan), must be stored frozen and the emulsion components mixed immediately before use. Recent formulations, such as PHER O_2 (Sanguine Corp, Pasadena, CA) are more stable and easier to handle. Regardless, it is difficult to attach targeting groups or other moieties to an emulsion droplet and conclusively track the PFC component in biological systems [11]. Nevertheless, despite the drawbacks of emulsions, the requirement of large payloads of PFC for detection using imaging techniques and for drug delivery lends itself to the use of stabilized droplets.

* Corresponding author at: Department of Tumor Immunology, Nijmegen Centre for Molecular Life Sciences, Radboud University Nijmegen Medical Centre, Postbox 9101, 6500 HB Nijmegen, The Netherlands. Tel.: +31 24 3617600; fax: +31 24 3540339.
E-mail address: J.deVries@ncmls.ru.nl (I.J.M. de Vries).

0142-9612/$ – see front matter © 2010 Elsevier Ltd. All rights reserved.
doi:10.1016/j.biomaterials.2010.05.069

Thus one key issue facing the successful development of fluorous imaging agents is the stability of the product in aqueous environments and for long-term storage. Furthermore, the ability to covalently bond targeting or other active agents, while retaining large PFC payloads is highly desirable. To address these needs, we propose a polymeric coating to encapsulate and stabilize the PFC, in place of a lipid coating. Biodegradable particles of poly(D,L-lactide-co-glycolide) (PLGA) have previously been used as carriers for controlled delivery of macromolecular therapeutics including proteins, peptides, vaccines, genes, antigens and growth factors [12–14]. The encapsulation technique has been applied to PFCs for use in ultrasound imaging, primarily to perfluorocarbon gases [15–17], with some work using perfluorocarbon liquids for ultrasound imaging [2]. Encapsulation in PLGA has several advantages including that PLGA is already FDA-approved for human use; PLGA is easily degraded and metabolized *in vivo*; PLGA formulations are stable for long-term storage; and PLGA particles can be targeted *in vivo* using antibodies or other ligands [18].

Here, we developed a stable formulation for a range of PFCs currently used in clinical and preclinical studies as imaging agents for MRI, CT and ultrasound. These PLGA-encapsulated PFC particles can be customized in terms of the diameter of the particle, the amount and type of PFC entrapped, inclusion of a fluorescent dye, surface charge and bound antibody. In this paper, we focused on the development of PLGA-encapsulated nanoparticle labels for cell tracking using ^{19}F MRI and fluorescence imaging, using encapsulated perfluoro-15-crown ether (PFCE). We used primary human dendritic cells (DCs), as used in cancer vaccination trials [19], as a model for cell labeling with these nanoparticles. Here, we demonstrate the use of the PLGA-encapsulated PFCs as a modular imaging label, focusing on cell tracking using ^{19}F MRI.

2. Materials and methods

2.1. Particle formulation and characterization

Particles were formulated and characterized as in [20], with the addition of PFCs as described here. Briefly, nanoparticles (200 nm diameter) with entrapped PFCs were prepared using PLGA (Resomer RG 502H, lactide: glycolide molar ratio 48:52–52:48; Boehringer Ingelheim, Ingelheim am Rhein, Germany) and a single emulsion technique using solvents dichloromethane, 2-propanol, N,N′-dimethylformamide and ethyl acetate (all from Merck, Darmstadt, Germany) and polyvinyl alcohol (Sigma, St. Louis, MO, USA) [17]. 90 mg of PLGA in 3 mL of methylene chloride containing distinct PFCs compounds, carboxyfluorescein (2 mg; Sigma, USA) or DyLight488 NHS-Ester or Atto 647 (both 0.5 mg, Thermo Scientific, Waltman MA, USA) were added dropwise to 25 mL of aqueous 2% (w/v) polyvinyl alcohol (PVA; Sigma, USA) and emulsified for 90 s using a sonicator (Sonifier 250; Branson Sonic Power, Danbury, CT, USA). Particles with a larger diameter (2000 nm) were prepared by double emulsion [21] using 90 mg of PLGA (Boehringer Ingelheim, Germany) in 1 mL of ethyl acetate containing PFCE and carboxyfluorescein (2 mg, Sigma, USA). All particles were washed extensively and lyophilized for 3–4 days.

Scanning electron microscopy was done on a Jeol JSM-6310 (Jeol Inc, Peabody, MA, USA). Dynamic light scattering was performed on an ALV light-scattering instrument equipped with an ALV5000/60X0 Multiple Tau Correlator and an Oxxius SLIM-532 150 mW DPSS laser operated at a wavelength of 532 nm (Langen, Germany). Zeta potential of particles was determined on a Malvern Zetasizer 2000 (Malvern, UK).

2.2. Surface modifications of the PLGA nanoparticles

The charge of the nanoparticles was modified by coating with DEAE-dextran and poly-L-lysine (Sigma, USA) using an o/w emulsion and solvent evaporation-extraction method. Briefly, 90 mg of PLGA in 3 mL of methylene chloride was added dropwise to 25 mL of aqueous 1.5% (w/v) polyvinyl alcohol (PVA; Sigma, USA) and 0.5% DEAE-dextran or 0.5% poly-L-lysine respectively, and emulsified for 90 s using a sonicator (Sonifier 250; Branson Sonic Power, Danbury, CT, USA). Next, after overnight evaporation at 4 °C, the nanospheres were collected by ultracentrifugation at 65 000 g for 30 min, washed three times with distilled water, and lyophilized for 3–4 days.

PLGA nanoparticles with mouse anti-human antibody against DC-SIGN (Alexion Pharmaceuticals, USA) on the surface and entrapped carboxyfluorescein (FITC; Sigma, USA) were prepared using a o/w emulsion and solvent evaporation-extraction. 50 mg of PLGA in 3 mL of methylene chloride containing 2 mg FITC was added dropwise to 25 mL of aqueous 2% (w/v) PVA in distilled water and sonicated for 90 s, as described in [20]. The presence of antibodies on the particle surface was confirmed by staining nanoparticles with goat anti-human secondary antibodies, followed by analysis on a FacsCalibur flow cytometer using CellQuest software (BD Biosciences, USA).

2.3. Cell culture and labeling

DCs were generated from adherent peripheral blood mononuclear cells (PBMC), from donor blood, by culturing in the presence of interleukin-4 (500 U/mL) and granulocyte–monocyte colony stimulating factor (800 U/mL) (both Cellgenix, Freiburg, Germany). Cells were cultured in X-VIVO 15 medium (BioWhittaker, Walkersville, MD) with 2% human serum (Bloodbank; Rivierenland, Nijmegen, The Netherlands). The indicated dose of PLGA particles was added at day 3. At day 6, the cells were matured by the addition of 10 μg/mL PGE_2 (Pharmacia & Upjohn, Puurs, Belgium), 10 ng/mL TNF-α, 5 ng/mL IL-1β and 15 ng/mL IL-6 (Cellgenix). On day 8, the cells were harvested using cold PBS, and then washed in PBS to remove excess particles. Cell viability was determined by trypan blue exclusion.

2.4. Confocal microscopy

Internalization of NP and MP containing carboxyfluorescein were confirmed by confocal microscopy. Cells were fixed on poly-L-lysine-coated glass slides and stained with anti-human MHC HLA-DR/DP class II antibody (clone Q5/13) or IgG2a isotype control, followed by a secondary mAb of goat anti-human Alexa 647 (all Molecular Probes, Eugene, OR, USA). Cells were imaged with a Bio-Rad MRC 1024 confocal system operating on a Nikon Optiphot microscope and a Nikon 60X planApo 1.4 oil immersion lens (Surey, UK).

2.5. Imaging

Mice were housed under specified pathogen-free conditions in the Central Animal Laboratory (Nijmegen, the Netherlands). All experiments were performed according to the guidelines for animal care of the Nijmegen Animal Experiments Committee.

MR imaging and spectroscopy was performed on a 7T MR system (Clinscan; Bruker Biospin, Ettlingen, Germany), equipped with a horizontal bore magnet (Ultra Shielded) and a gradient system with 20 cm inner diameter and maximum gradient strength of 300 mT/m. Imaging of PFCs *in vitro* (Fig. 2) was done using a ^{19}F TSE (turbo factor 12), TR/TE of 5000/6 ms, resolution of 0.12 × 0.12 × 1 mm and a bandwidth of 300 Hz/pixel. The ^{19}F frequency was centered on each peak or group of peaks individually. ^{19}F FIDs were acquired with a TR of 5000 ms and a bandwidth of 50,000 Hz. A 10 mm diameter ^{1}H/^{19}F surface coil was used.

In vivo imaging (Fig. 4) was done using a ^{1}H/^{19}F volume coil for the mouse leg. A TSE sequence was used for ^{1}H, with TR/TE of 1500/14 ms, 0.12 × 0.6 × 2 mm voxels and 8 averages. For ^{19}F, we used a GRE sequence with TR/TE of 200/2.82 ms, a 20° flip angle and 1.88 × 0.94 × 2 mm voxels with 512 averages (27 min). For *in vivo* imaging, C57B/l6 (Charles River Wiga, Sutzfeld, Germany) female mice were injected in the footpad with 10 mg of PLGA particles containing PFCE (particle #4) or labeled cells. The mice were anesthetized with an i.v. injection of ketamine (Nimatek, Eurovet Animal Health B.V., Bladel, the Netherlands) and dexmedetomidine (Dexdomitor, Orion-Pharma, Hamburg, Germany). Body temperature was monitored and regulated during imaging. The imaging parameters for the mouse images in Fig. 5 were TR/TE of 1000/3.5 ms, 0.125 × 0.125 × 10 mm voxels, 16 averages and a turbo factor of 16. For ^{19}F, TR/TE was 700/3.5 ms, 0.5 × 0.5 × 10 mm voxels with 500 averages and a turbo factor of 4. The parameters for the tubes (Fig. 5) were similar, except that the voxel size was 0.15 × 0.15 × 10 mm with 1 average for ^{1}H and 0.65 × 0.65 × 10 mm with 300 averages for ^{19}F.

Magnetic resonance spectrometry was used to measure the ^{19}F content per cell. Labeled cell pellets were placed in sealed tubes with a reference sample of 100 μL of 0.5% solution of trifluoroacetic acid (TFA). The respective spectral weights was measured and compared to determine the ^{19}F content per cell.

For fluorescence imaging, mice or sample tubes were placed in a FluorVivo 300 (INDEC BioSystems, Santa Clara, CA USA). Exposure times were between 0.05 and 0.15 s.

3. Results

3.1. Creating customized PFC/PGLA particles optimized for ^{19}F MRI

Several PFCs are in clinical and preclinical use. These compounds are generally emulsified to stabilize them in aqueous environments, but here we encapsulated PFCs in a hydrophilic PLGA polymer. We studied the ^{19}F NMR spectra (Fig. 1) and determined the entrapment efficiency in PLGA particles when equal weights of each PFC were added to the PLGA (Table 1). For ^{19}F MRI, a single resonance peak, as with the PFCE, is desirable in order to minimize chemical shift artefacts (Fig. 1e). Table 1 summarizes data

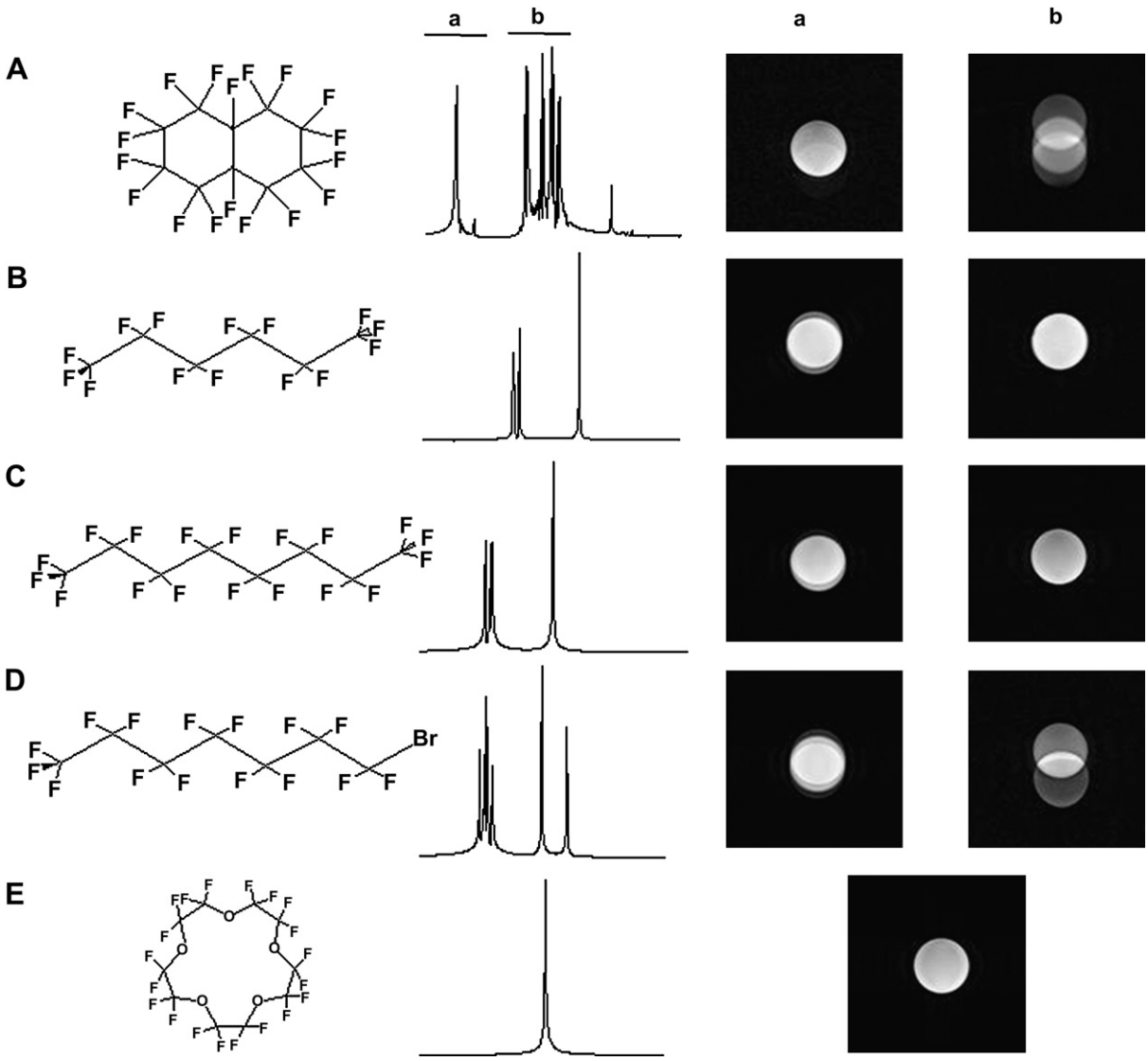

Fig. 1. ^{19}F NMR spectrum and molecular structure of various PFCs. The ^{19}F NMR spectrum, chemical structure and the ^{19}F MR images are shown. The acquisition frequency of the MR images was centered on each peak or group of peaks, and the corresponding image is shown (indicated by *a* and *b*). (A) Perfluorodecalin ($C_{10}F_{18}$) has several peaks in the ^{19}F spectrum. It is used in commercial oxygen carriers and blood pool agents. (B) Perfluorohexane (C_6F_{14}) is also used as a contrast agent for ultrasound imaging. (C) Perfluorooctane (C_8F_{18}) is also used as an oxygen carrier. (D). Perfluorooctylbromide (C_8BrF_{17}), or PFOB, is a blood substitute that has also been used for ^{19}F MRI. However, the presence of multiple ^{19}F resonances complicates the imaging process. (E) Perfluoro-15-crown ether ($C_{10}F_{20}O_5$) has 20 equivalent ^{19}F atoms, resulting in a single resonance peak. The compound has been used for ^{19}F MRI for cell tracking and as an oxygen sensor.

from encapsulation of these PFCs in PLGA showing the entrapment efficiency, particle diameter and surface charge or zeta potential. All the particles range from 200 to 300 nm in diameter and are monodisperse, as indicated by the low poly dispersity index (PDI). The zeta potential of the particles is between −41 and −49 mV, largely due to the negatively charged PLGA. We focused on the PFCE in all further experiments as it has a single NMR resonance and presented the highest encapsulation in PLGA when compared with the other PFCs.

The particle is depicted as a cartoon in Fig. 2a, summarizing its main characteristics. Fig. 2b shows electron micrographs for PFCE particles of different sizes. The size of the PLGA particles produced can be varied depending on the formulation conditions (see Methods). Preliminary cell labeling studies were carried out using PFCE particles conjugated to a fluorescent dye (Fig. 2c). Both the larger and smaller particles (2000 and 200 nm diameter) were taken up efficiently and localized intracellularly, with a diffuse cytoplasmic distribution. No other morphological differences were observed between labeled and non-labeled DCs. Based on these results, we decided to use the smaller particles (200 nm diameter) as they showed higher PFCE encapsulation. To demonstrate the ability to manipulate the external surface of the particles, we increased the charge by coating with positively charged oligomers (Fig. 2d) and covalently bound an antibody targeting a DC surface marker (Fig. 2e).

PFCE encapsulation in the PLGA nanoparticles was optimized (Fig. 2f), by adding an increasing amount of PFCE during particle synthesis. The encapsulation of PFCE increases until particle #5, where roughly 3.5-fold as much PFCE as PLGA was added. A sharp drop in encapsulation occurs at higher concentrations of PFCE. The particle size remained between 225 and 260 nm, regardless of the amount of PFCE encapsulated. A representative particle size distribution is shown in Fig. 2g, from particle #4. All of the particles showed a single peak and a low PDI, indicating a single population (Supplementary Table 1).

Table 1
Particle characteristics. PLGA particles encapsulate different PFCs with an entrapment efficiency between 3 and 12% when equal weights of the PFC were added during particle formulation. The diameters range from 220 to 318 nm with a low poly dispersity index (PDI), and a relatively constant zeta potential of about −45 mV. Of the PFCs selected all except for the PFCE have been used clinically as oxygen carriers or ultrasound imaging agents ($n = 3$).

Compound	Entrapment efficiency (% w/w)	Diameter ± S.D. (nm)	PDI ± S.D.	Zeta potential (mV)
perfluorodecalin	7.6 ± 1.9	286 ± 16	0.20 ± 0.03	−44 ± 2
perfluorohexane	3.1 ± 1.1	266 ± 10	0.06 ± 0.01	−49 ± 2
perfluorooctane	5.2 ± 1.9	220 ± 6	0.26 ± 0.02	−49 ± 2
Perfluorooctylbromide	7.7 ± 1.2	272 ± 12	0.34 ± 0.02	−41 ± 2
Perfluoro-15-Crown-5-Ether	12 ± 0.6	318 ± 14	0.25 ± 0.02	−41 ± 1

In conclusion, particle #5, where 3.2 mg of PFCE was added per mg of PLGA during synthesis encapsulated the highest amount of PFCE (422 ± 50 μg PFCE/mg PLGA) with a diameter of 239 ± 4 nm. In our subsequent experiments, we focused on this particle and particle #4.

3.2. Labeling primary human DCs with the PFC/PLGA nanoparticles

We tested the ability of primary human DCs to take up the nanoparticles. PLGA nanoparticles were added at 0–20 mg of PLGA to immature DCs. Initial studies were performed using PFCE-

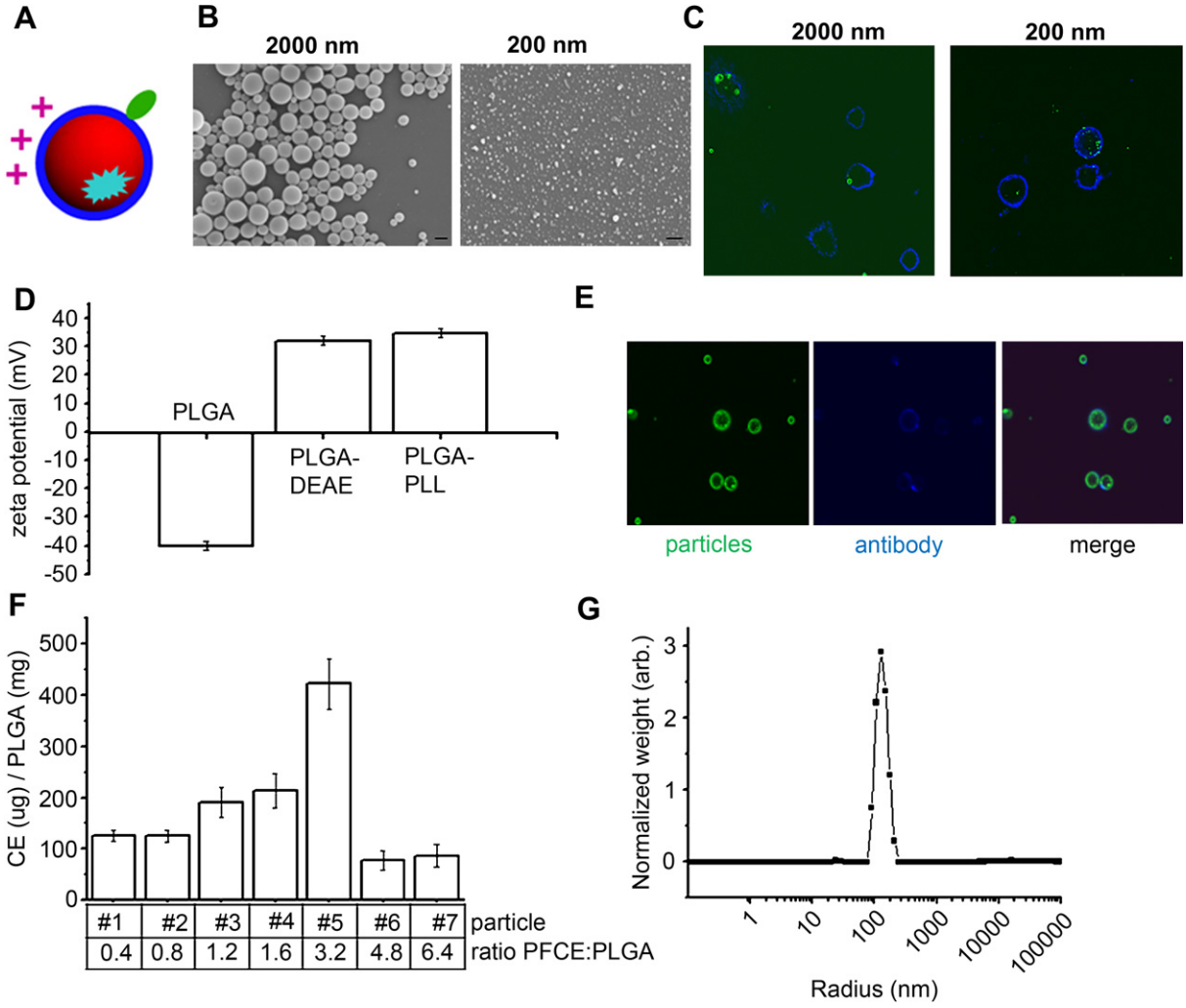

Fig. 2. Multi-functional PFCE-PLGA particles. (A) A cartoon of particle design. The PFC of choice (red) is encapsulated within the PLGA coating (blue). Other compounds of interest, such as drugs or fluorescent dyes, can also be encapsulated (cyan). The PLGA can be coated with various surface agents to vary the charge (purple) or for other functions, such as targeting or dyes (green). The size of the particle can also be varied from about 200 to 2000 nm. Finally, the lifetime of the particle can be varied, by adjusting the PLGA composition, solvents and preparation. (B) Scanning electron micrographs of two different PFCE particles are shown. The scale bar represents 1 μm. (C) Confocal images of cells labeled with particles of different sizes, at 2000 and 200 nm. The particles are labeled with carboxyfluorescein (green), and the cell membrane is visualized by MHC II staining (blue). The image represents a central focal plane of the DCs. The particles are clearly intracellular, at both sizes. (D) The zeta potential of the particles can be increased by the addition of positively charged coatings, such as DEAE-dextran and poly-L-lysine. (E) The particles can also be bound to an antibody, as shown in the fluorescence images where the particles (green) overlap with the antibody (blue), detected using a secondary fluorescent antibody. (F) PFCE content for particles 1–7, all with a diameter around 250 nm. The highest PFCE content was with particle #5, at 0.42 μg/mg PLGA. (G) A representative particle diameter distribution for particles 1–7, obtained using DLS. All the particles show a single peak with a low PDI of 0.1–0.2.

containing particles with FITC (Fig. 2c). Particles #4 and #5 were tested at various doses with primary human DCs (Fig. 3a). Fig. 3b shows that the ^{19}F cell loading with particle #4 was lower than with #5. Reanalyzing this data for viability versus PFCE added (without differentiating between nanoparticles; Fig. 3c), indicates that 2500 μg PFCE per million cells is the maximal tolerable dose for DCs, under these labeling conditions.

Taken together, Particle #4 resulted in the highest label uptake and cell viability (2.5×10^{13} F atoms per cell, nearly 100% viability), relative to untreated controls. Under these conditions, no changes to the expression of DC markers CD80, CD83, CD86 and CCR7 relative to non-labeled cells were found (Supplementary information Fig. 1).

In order to study the stability of particle #4 under our cell labeling conditions, we incubated the nanoparticles in PBS at 37 °C for up to 48 h (Supplementary Table 2). Diameter is a measure of the stability of particles, and this remained invariant. The particle size remained stable over a period of at least 48 h, suggesting that the nanoparticles are stable for the duration of the labeling process.

Finally, we tested the sensitivity of fluorescence imaging and MRI using known numbers of DCs labeled with nanoparticles with both PFCE and a far-red fluorescent dye (Fig. 3d). This demonstrates that the DCs can be dual-labeled for both imaging modalities.

3.3. *In vivo imaging*

In order to demonstrate that the PFCE nanoparticles contain sufficient ^{19}F for detection by *in vivo* MRI, we imaged particle #4 *in vivo* (Fig. 4). We also imaged labeled cells in a similar manner (Fig. 5). This particle showed high PFCE encapsulation and low toxicity (Fig. 3). 10 mg of nanoparticles were injected in a mouse footpad, and we acquired a ^{19}F image at a spatial resolution of $1.88 \times 0.94 \times 2$ mm, using a standard gradient echo sequence within 27 min, with a signal to noise ratio (SNR) of 3.4 at 7T. Mice were imaged immediately after injection of nanoparticles (0 h) and 7 days later. The ^{19}F signal decreased significantly over this time period, indicating clearance of the nanoparticles from the injection site. No side effects were observed in the mice up to 1 week post-injection.

3 million DCs labeled using PLGA nanoparticles with a far-red dye and PFCE were injected in a similar manner and imaged with MR and fluorescence imaging (Fig. 5). The other footpad received similar nanoparticles with a green dye and crown ether. Nanoparticles and labeled cells could be detected with both imaging modalities. Thus, we conclude that the nanoparticles contain sufficient PFCE and are suitable for dual-modality *in vivo* imaging.

4. Discussion

We have shown the versatility of the PLGA particles, their ability to label primary human DCs and their utility for *in vivo* imaging. These particles can be customized in terms of the encapsulated contents (PFC, dyes and/or drugs, for example), particle size, charge and bound moiety. We applied these particles with a PFCE payload to the labeling of primary human DCs for ^{19}F MRI and fluorescence imaging.

Pervious work using perfluorocarbons to label cells focused on emulsions. For example, using PFCE emulsified with lipid surfactants [22,23]. Other emulsions used as cell labels have focused on linear PFPEs, also emulsified in lipids [7,8,11]. The lipid surfactants used in these studies range from egg phospholipids to pluronics, and transfection agents may be used to improve cellular uptake. In general, surfactants are miscible with both phases of the emulsion; however this is not the case with these PFC emulsions. Interactions between PFCs and hydrocarbons are inherently weak, leading to instability. Aging of these emulsions occurs primarily through

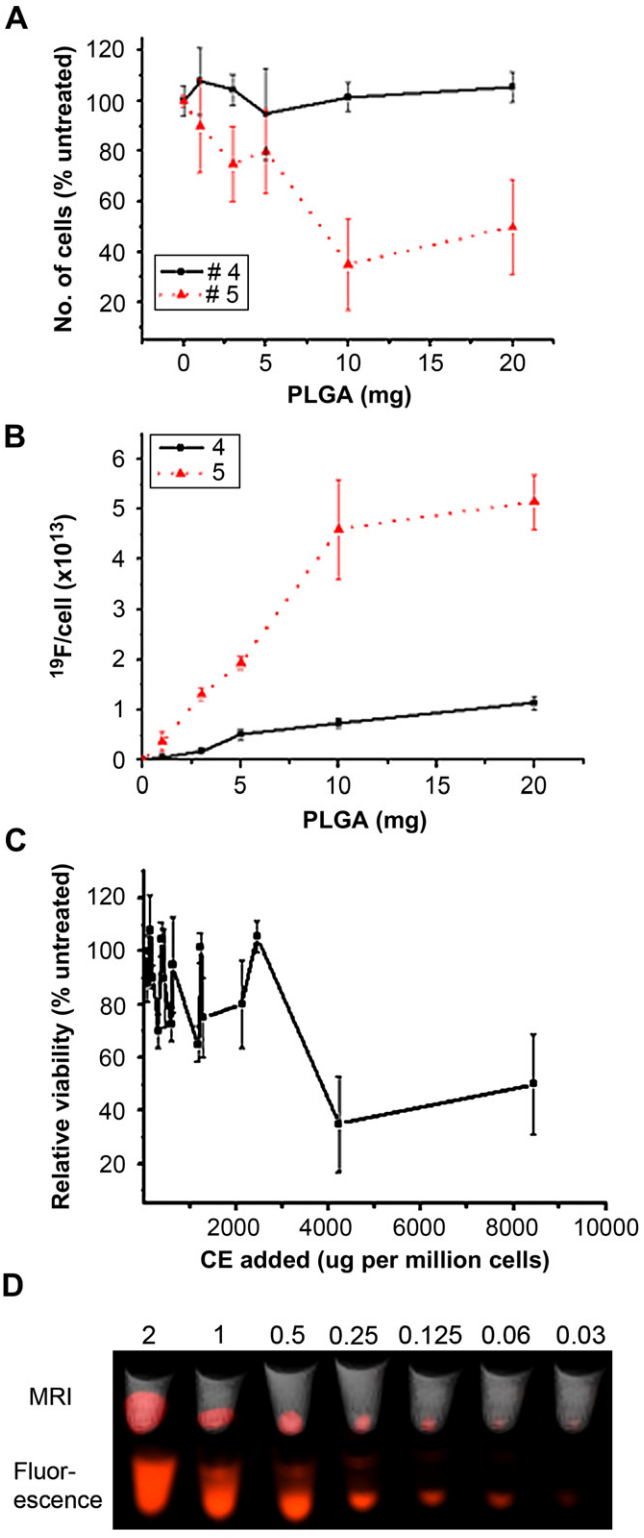

Fig. 3. Labeling primary human dendritic cells with PFCE particles. (A) Toxicity with a dose curve for particles #4,5,7 expressed as number of cells (% untreated control) vs. mg of PLGA added. Particle 5 showed the highest toxicity at concentrations over 5 mg (B) ^{19}F per cell for particles #4 and5 at different concentrations added to the cells. Particle 5 showed the highest uptake of PFCE. (C) Cell viability plotted as a function of PFCE uptake. The DCs remained viable until about 2500 μg of PFCE added. (D) DCs labeled with PLGA containing PFCE and a fluorescent dye were imaged with MR and fluorescence imaging. The numbers indicate the number of cells in millions.

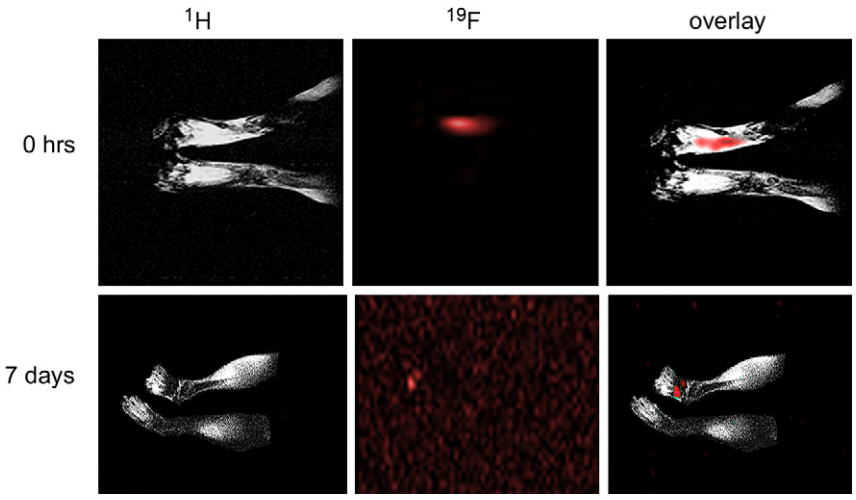

Fig. 4. MR image showing PFCE particles. The mouse was injected with particle #4 in one footpad, and the mouse imaged immediately (0 h) and 7 days later. The images shown are 2 mm coronal slices with ^{1}H in grayscale, ^{19}F in false color and an overlay. The particles are clearly visible at the injection site, although the signal is diminished by day 7. The acquisition time for the ^{1}H TSE scan was 15 min and the ^{19}F GRE was 27 min.

coalescence and Ostwald ripening [24], over a period of hours to several days unless stored at low concentrations. Nevertheless, despite the unstable attraction between the surfactant and the PFC, such emulsions have been successfully used in targeting studies [25].

The use of PLGA encapsulation allows for the stabilization of the PFCs without the need for emulsification. This results in a stable product that can be lyophilized or solubilized in water or buffer and frozen for storage. Due to this convenience and their ready uptake by macrophages and DCs, PLGA particles have been extensively studied for antigen delivery [26]. Furthermore, the particle size can be controlled, and a narrow size distribution can be achieved (Fig. 2g). Another major advantage is that the PLGA particles present a stable surface for the addition of targeting agents, such as antibodies [reviewed in [27]]. PLGA particles have also been used for gene transfection [reviewed in [28]]. Degradation of the particles occurs via bulk erosion, the rate of which can be controlled by varying the size of the polymer and formulation [29]. From the literature, it is thought that PLGA particles are able to escape lysosomes and thus largely bypass intracellular degradation [30]. The PLGA monomers themselves, lactic and glycolic acid, are cleared by the Krebs cycle. These monomers can result in an acidic environment within the particles, in the range of pH 1.5–3 [29]. However, PFCs such as the PFCE are stable at low pH values as the C–F bond is not degraded *in vivo*. Indeed, PFCs have been found to be biologically compatible even at the high doses used in blood substitutes. It is known that these compounds are cleared through exhalation from the lungs [31]. The PLGA particles are also stable for long-term storage when frozen or lyophilized [2], [26]. In solution, the nanoparticles are stable for at least 48 h at 37 °C (Supplementary Table 2).

The nanoparticles showed minimal toxicity with primary human DCs, even at concentrations as high as 20 mg per million cells (Fig. 3a). Furthermore, we did not observe any effect of labeling on cell function, in terms of migration or expression of maturation markers (Supplementary information Fig. 1). The ^{19}F loading per cell is also similar to previous work using DCs labeled with PFC emulsions and transfection agents [23]. However, the

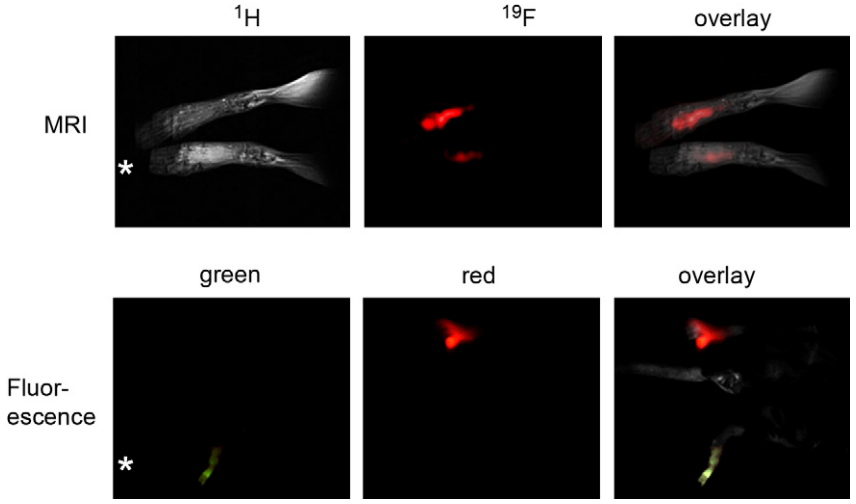

Fig. 5. Fluorescence and MR images of labeled DCs and PLGA particles. 3 million DCs labeled with particles with PFCE and a far-red dye were injected in one footpad of a mouse and PFCE particles with a green dye in the other (asterix). Upper panels shows the MR images (^{1}H in grayscale, ^{19}F in false color and an overlay), and the lower panels the fluorescence images.

PLGA nanoparticles in our study bypassed the need for transfection agents to achieve sufficient ^{19}F loading. This is a major advantage as transfection agents are generally not clinically applicable. Furthermore, ^{19}F loading using PFCs together with transfection agents may affect cell function, for example by a reduction of surface marker expression [7]. The use of positively charged PFCE nanoparticles (Fig. 2c) could increase uptake in cells that are not phagocytic, such as T cells, simulating the effect of a transfection agent. The use of relevant antibodies (Fig. 2e) can also be used to increase cell labeling or for *in vivo* targeting [20].

All the PFCE nanoparticles, #1–7, were able to label the DCs, but the highest labeling was achieved with #5, which was also the most toxic to DCs (Fig. 3). As particle #5 has the highest amount of encapsulated PFCE, at nearly 0.5 μg/mg PLGA, it may be better suited for applications that do not require cell labeling, such as blood pool imaging agents. PFCE itself is generally thought to be inert and therefore non-toxic within biological systems. In keeping with this observation, we did not observe any effect on mice after injection with these nanoparticles for up to 7 days post-injection. Furthermore, the ^{19}F signal in the injection site decreased within this period indicating that the PLGA nanoparticles are cleared from the site of transfer.

Finally, although we focused here on cell labeling for MRI, PFCs have been used for ultrasound and CT contrast [1,2]. PLGA particles are also versatile- targeting groups, charged compounds, dyes, drugs or other agents can be either directly coupled to the PLGA or encapsulated within the fluorous core [3]. PLGA particles have been used for controlled drug delivery [reviewed in [13]], where the addition of a tracking agent, such as a PFC for ^{19}F MRI, would allow the tracking of the drug *in vivo*.

5. Conclusions

Here, we have demonstrated some of the versatility of the PLGA-encapsulated PFCs as a modular imaging label. The main strength of this system is that it can readily be adapted to the requirements of each study. For example, we showed that the addition of a fluorescent dye to the particles allows *in vivo* fluorescence imaging (Fig. 5), and flow cytometric and histological analyses of labeled cells after transfer to the subject. Additional applications include ultrasound, CT contrast and drug delivery. Particle size, charge and coating can also be modified to suit the intended use (Fig. 2). Clinical trials such as those involving cell vaccinations would benefit greatly from the application of a quantitative *in vivo* imaging modality, such as ^{19}F MRI. We suggest that PLGA encapsulation is a suitable method for stabilizing PFCs in aqueous environments for a myriad of *in vivo* imaging and targeting applications.

Acknowledgements

We would like to thank Kim Kweldam and Mathieu Somers for their assistance with the anesthetics for MRI; and Peter Friedl, Gert-Jan Bakker and Michiel van Dommelen for assistance with fluorescence imaging. This research was supported by EU grant ENCITE (HEALTH-F5-2008-201842), NWO Vidi grant 917.76.363 to JdV and EU grant Immunanomap (MRTN-CT-2006-035946). This work was also supported by investment grants NWO middelgroot nr 40-00506-90-06021 and NWO BIG (VISTA).

Appendix. Supplementary data

The supplementary data associated with this article can be found in the on-line version at doi:10.1016/j.biomaterials.2010.05.069.

Appendix

Figures with essential color discrimination. Figs. 2–5 in this article are difficult to interpret in black and white. The full color images can be found in the on-line version, at doi:10.1016/j.biomaterials.2010.05.069.

References

[1] Mattrey RF. The potential role of perfluorochemicals (PFCs) in diagnostic imaging. Artif Cells Blood Substit Immobil Biotechnol 1994;22(2):295–313.
[2] Pisani E, Tsapis N, Paris J, Nicolas V, Cattel L, Fattal E. Polymeric nano/microcapsules of liquid perfluorocarbons for ultrasonic imaging: physical characterization. Langmuir 2006;22(9):4397–402.
[3] Lanza GM, Winter PM, Neubauer AM, Caruthers SD, Hockett FD, Wickline SA. 1H/19F magnetic resonance molecular imaging with perfluorocarbon nanoparticles. Curr Top Dev Biol 2005;70:57–76.
[4] Kodibagkar VD, Wang X, Mason RP. Physical principles of quantitative nuclear magnetic resonance oximetry. Front Biosci 2008;13:1371–84.
[5] Procissi D, Claus F, Burgman P, Koziorowski J, Chapman JD, Thakur SB, et al. In vivo 19F magnetic resonance spectroscopy and chemical shift imaging of trifluoro-nitroimidazole as a potential hypoxia reporter in solid tumors. Clin Cancer Res 2007;13(12):3738–47.
[6] Srinivas M, Heerschap A, Ahrens ET, Figdor CG, Vries IJ. (19)F MRI for quantitative in vivo cell tracking. Trends Biotechnol; 2010 Apr 26 [Epub ahead of print].
[7] Srinivas M, Morel PA, Ernst LA, Laidlaw DH, Ahrens ET. Fluorine-19 MRI for visualization and quantification of cell migration in a diabetes model. Magn Reson Med 2007;58(4):725–34.
[8] Srinivas M, Turner MS, Janjic JM, Morel PA, Laidlaw DH, Ahrens ET. In vivo cytometry of antigen-specific t cells using (19)F MRI. Magn Reson Med 2009;62(3):747–53.
[9] Riess JG. Understanding the fundamentals of perfluorocarbons and perfluorocarbon emulsions relevant to in vivo oxygen delivery. Artif Cells Blood Substit Immobil Biotechnol 2005;33(1):47–63.
[10] Riess JG, Postel M. Stability and stabilization of fluorocarbon emulsions destined for injection. Biomater Artif Cells Immobilization Biotechnol 1992;20 (2–4):819–30.
[11] Janjic JM, Srinivas M, Kadayakkara DK, Ahrens ET. Self-delivering nanoemulsions for dual fluorine-19 MRI and fluorescence detection. J Am Chem Soc 2008;130(9):2832–41.
[12] Caputo A, Sparnacci K, Ensoli B, Tondelli L. Functional polymeric nano/microparticles for surface adsorption and delivery of protein and DNA vaccines. Curr Drug Deliv 2008;5(4):230–42.
[13] Mohamed F, van der Walle CF. Engineering biodegradable polyester particles with specific drug targeting and drug release properties. J Pharm Sci 2008;97 (1):71–87.
[14] Vasir JK, Labhasetwar V. Biodegradable nanoparticles for cytosolic delivery of therapeutics. Adv Drug Deliv Rev 2007;59(8):718–28.
[15] Cui W, Bei J, Wang S, Zhi G, Zhao Y, Zhou X, et al. Preparation and evaluation of poly(L-lactide-co-glycolide) (PLGA) microbubbles as a contrast agent for myocardial contrast echocardiography. J Biomed Mater Res B Appl Biomater 2005;73(1):171–8.
[16] Goldberg SN, Walovitch RC, Straub JA, Shore MT, Gazelle GS. Radio-frequency-induced coagulation necrosis in rabbits: immediate detection at US with a synthetic microsphere contrast agent. Radiology 1999;213(2):438–44.
[17] Pisani E, Fattal E, Paris J, Ringard C, Rosilio V, Tsapis N. Surfactant dependent morphology of polymeric capsules of perfluorooctyl bromide: influence of polymer adsorption at the dichloromethane-water interface. J Colloid Interface Sci 2008;326(1):66–71.
[18] Acharya S, Dilnawaz F, Sahoo SK. Targeted epidermal growth factor receptor nanoparticle bioconjugates for breast cancer therapy. Biomaterials 2009;30 (29):5737–50.
[19] de Vries IJ, Lesterhuis WJ, Barentsz JO, Verdijk P, van Krieken JH, Boerman OC, et al. Magnetic resonance tracking of dendritic cells in melanoma patients for monitoring of cellular therapy. Nat Biotechnol 2005;23(11):1407–13.
[20] Cruz LJ, Tacken PJ, Fokkink R, Joosten B, Stuart MC, Albericio F, et al. Targeted PLGA nano- but not microparticles specifically deliver antigen to human dendritic cells via DC-SIGN in vitro. J Contr Release 2010;44(2):118–26.
[21] Jain RA. The manufacturing techniques of various drug loaded biodegradable poly(lactide-co-glycolide) (PLGA) devices. Biomaterials 2000;21(23): 2475–90.
[22] Partlow KC, Chen J, Brant JA, Neubauer AM, Meyerrose TE, Creer MH, et al. 19F magnetic resonance imaging for stem/progenitor cell tracking with multiple unique perfluorocarbon nanobeacons. FASEB J 2007;21(8):1647–54.
[23] Ahrens ET, Flores R, Xu H, Morel PA. In vivo imaging platform for tracking immunotherapeutic cells. Nat Biotechnol 2005;23(8):983–7.
[24] Freire MG, Dias AM, Coelho MA, Coutinho JA, Marrucho IM. Aging mechanisms of perfluorocarbon emulsions using image analysis. J Colloid Interface Sci 2005;286(1):224–32.
[25] Waters EA, Chen J, Allen JS, Zhang H, Lanza GM, Wickline SA. Detection and quantification of angiogenesis in experimental valve disease with integrin-

targeted nanoparticles and 19-fluorine MRI/MRS. J Cardiovasc Magn Reson 2008;10(1):43.
[26] Waeckerle-Men Y, Groettrup M. PLGA microspheres for improved antigen delivery to dendritic cells as cellular vaccines. Adv Drug Deliv Rev 2005;57 (3):475–82.
[27] Panyam J, Labhasetwar V. Targeting intracellular targets. Curr Drug Deliv 2004;1(3):235–47.
[28] Abbas AO, Donovan MD, Salem AK. Formulating poly(lactide-co-glycolide) particles for plasmid DNA delivery. J Pharm Sci 2008;97(7):2448–61.
[29] Houchin ML, Topp EM. Chemical degradation of peptides and proteins in PLGA: a review of reactions and mechanisms. J Pharm Sci 2008;97 (7):2395–404.
[30] Cartiera MS, Johnson KM, Rajendran V, Caplan MJ, Saltzman WM. The uptake and intracellular fate of PLGA nanoparticles in epithelial cells. Biomaterials 2009;30(14):2790–8.
[31] Flaim SF. Pharmacokinetics and side effects of perfluorocarbon-based blood substitutes. Artif Cells Blood Substit Immobil Biotechnol 1994;22(4): 1043–54.